Geometry Optimization of a Continuous Millireactor via CFD and Bayesian Optimization[†]

Moritz J. Begall,[‡] Artur M. Schweidtmann,[‡,¶] Adel Mhamdi,[‡] and Alexander Mitsos[*,‡,§]

‡*RWTH Aachen University, Aachener Verfahrenstechnik – Process Systems Engineering (AVT.SVT), 52074 Aachen, Germany*

¶*Delft University of Technology, Department of Chemical Engineering, Delft 2629 HZ, The Netherlands*

§*Forschungszentrum Jülich GmbH, Institute of Energy & Climate Research IEK-10, 52425 Jülich, Germany*

E-mail: amitsos@alum.mit.edu

[†]This is the Authors' Accepted Manuscript of the following article: M. J. Begall, A. M. Schweidtmann, A. Mhamdi, A. Mitsos, Geometry optimization of a continuous millireactor via CFD and Bayesian optimization, Computers & Chemical Engineering 171, pp. 108140, 2023, which has been published in final form at https://doi.org/10.1016/j.compchemeng.2023.108140.

Abstract

Computational Fluid Dynamics (CFD) is a powerful tool which can help with the geometry optimization of continuous milli-scale reactors, which often are highly complex devices. Attempting to perform this optimization by manually modifying and testing geometry configurations can however be tedious and computationally inefficient. Addressing this problem, we present a framework in which the CFD software COMSOL Multiphysics is coupled with the multi-objective Bayesian Optimization algorithm TSEMO (Thompson sampling efficient multiobjective optimization), implemented in MATLAB. The mixing element geometry of a Miprowa Lab millireactor is parameterized, and the framework automatically executes CFD simulations to minimize areas of stagnating flow and maximize the mixing performance. The framework is able to find Pareto-optimal reactor variations, and can easily be adapted for other devices and objectives.

1 Introduction

Polymerization processes in the (specialty) chemical industry increasingly rely on continuous flow processing[1–6]. Continuous polymerization reactors are promising, because their large surface to volume ratio allows for faster heat removal and better temperature control than batch reactors[7,8]. Furthermore, this ratio can be kept constant during scaleup, reducing the need for pilot stages making it easier to go from lab- to production scale[9]. However, continuous polymerization reactors, especially milli-scale reactors with internal mixing elements, can be highly complex devices, which can be difficult to characterize experimentally, as many of their properties are not readily available via measurements. Additionally, their small size renders them especially prone to fouling[10,11].

Computational fluid dynamics (CFD) can be a useful tool to overcome these challenges and understand fouling, and is increasingly being used to study milli- and microscale devices[12–23]: Firstly, it enables the evaluation of flow process properties at arbitrary points

inside the computational domain, thus offering a look into the reactor. Secondly, it provides a way to evaluate the effect of modifications to the reactor design or process parameters.

In previous work, we employed CFD successfully to find geometry modifications which reduced the fouling potential in the Miprowa Lab millireactor [24]. However, we only considered manual specification of modifications which requires a lot of user input and we did not allow for configurations strongly deviating from the original design. We thus herein propose to overcome these challenges by coupling the CFD solver with a suitable optimization algorithm.

Optimization algorithms can generally be divided into gradient-based and gradient-free methods [25]. Gradient-based methods require the evaluation of the derivatives of the objective and constraint function(s) with respect to the design parameters. In principle, these can be calculated via sensitivities or adjoints, propagated through the CDF calculations, see e.g. [26,27]. In many cases, such as when dealing with proprietary software where the source code is not available, the derivatives are however inaccessible. It is indeed possible to approximate the derivatives of such black-box functions via finite differences, but this is expensive computationally, as each function evaluation corresponds to the solution of a CFD simulation. On the other hand, gradient-free methods often require a very large number of iterations, again resulting in high computational cost. Bayesian Optimization is a gradient-free method suitable for expensive black-box evaluations (via small number of required function evaluations) [25,28].

Combining Bayesian optimization with CFD for geometry design and shape optimization is becoming increasingly popular, see e.g. [25,29,30], but still a relatively new approach. In the area of chemical reactor design, optimizations have been reported e.g., for stirred tank reactors, [31] fluidized bed reactors, [32] and liquid-phase jet reactors, [33] but overall, few studies have been reported thus far. In particular, to our knowledge, no studies describing continuous flow reactors with internal mixing elements have been investigated in previous works. Due to their particularly complex geometries, these types of reactors represent especially interesting and challenging applications.

We present a framework in which the CFD software COMSOL Multiphysics [34,35] is cou-

pled with the Bayesian Optimization algorithm TSEMO (Thompson sampling efficient multiobjective optimization)[36,37], implemented in MATLAB. The mixing element geometry of a Miprowa millireactor[24,38,39] is parameterized, and the framework automatically runs and evaluates CFD studies to minimize areas of stagnating flow and maximize the mixing performance. The framework is able to find Pareto-optimal reactor variations, and can easily be adapted for other devices and objectives. Our work shows that Bayesian optimization and CFD can be applied successfully to complex devices like continuous flow milliscale mixers and reactors. Further, by quantifying the improvements that can be achieved, and the tradeoffs that have to be made, it enables a more meaningful discussion about the merits and limits of geometry optimization in this context.

2 Methods

In this section, we discuss the models and methods used, starting with a description of the millireactor, explaining the objective functions used for the optimization, and describing the CFD setup, the optimization method and their coupling.

2.1 Millireactor model

The Miprowa Lab millireactor was developed by Ehrfeld Mikrotechnik[40]. It was designed for single- or multiphase liquid-liquid or liquid-gas applications, can be operated at a wide range of temperatures and pressures, and has an effective fluid volume of about 20 mL. The reactor contains eight identical process channels, which are arranged in series, and can be heated or cooled by an enveloping thermal fluid. The individual channels are rectangular, with an interior cross-section of 12 mm by 1.5 mm and a length of 300 mm. They contain three layers of mixing elements, forming a three-dimensional herringbone pattern. The general form of a reactor channel is shown in Figure 1. The rectangular form (as opposed to round) is chosen by Ehrfeld Mikrotechnik for two reasons: *i* the surface area of the channels is larger,

enhancing heat transfer; *ii* the structure of the mixing elements is simpler, making their manufacture comparatively simple. This allows for the use and even adaptation of different elements, depending on the specific reactor application.

We shortened the channel to L=50 mm to speed up the computation time. This should not qualitatively impact the results because of the periodicity of the design and the fact that the impact of the inlet section on the velocity field is small, leading to well-developed flow even shortly after the inlet (cf. left side of Figure 2). The shape of the channel is determined by the angle of the mixing element fins α, the thickness of the fins d and their distance s (cf. Figure 1). We consider these parameters as the optimization variables.

The optimizations use three reference configurations as a starting point, all sharing a fin thickness of $d = 1\,\text{mm}$ and a fin distance of $s = 2\,\text{mm}$, with angles of $\alpha = 30°$, $\alpha = 45°$ and $\alpha = 60°$, respectively. To ensure that the configurations proposed by the optimization algorithm still bear a meaningful resemblance to the original geometries, and still consist of a single, well-connected domain, we impose the following bounds on the parameters: The angle α is allowed to vary between 15° and 75°, and d and s both can take a minimum value of 0.5 mm and a maximum value of 2.5 mm.

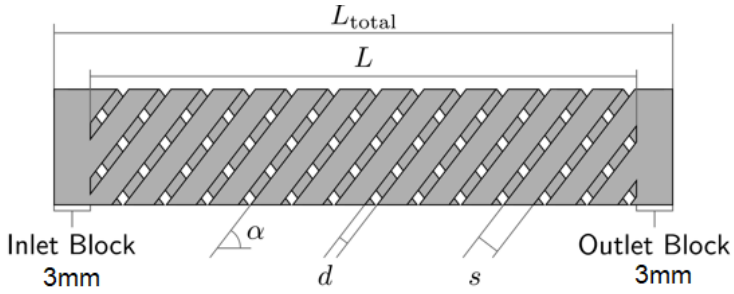

Figure 1: The geometry and parameters of the reactor. Shown is the effective interior volume, i.e. the volume taken up by the fluid; the gaps are the space taken up by the mixing elements.

2.2 Objective functions

We optimize the reference geometry of the Miprowa millireactor with respect to two competing objectives: The areas in which stagnating flow occurs, and the mixing variance, which are to be minimized. We explain these optimization objectives and the rational behind our choice in some detail in the following sections.

2.2.1 Minimize stagnating flow

Areas with stagnating flow can be prone to fouling[41], and should thus be minimized as far as possible. Since there is no clearly established definition of when a flow is said to be stagnant, in the present work we regard a velocity magnitude $|\boldsymbol{v}|$ of 5 % of the inlet velocity v_{in} as the cutoff point, and all points in the domain with this value or less are designated stagnant. This is expressed in the weight function $W(\boldsymbol{v})$ (see Equation(1)). We then integrate over the computational domain, and divide by the volume of the domain V, to get a dimensionless number for the magnitude of stagnating areas. This magnitude is denoted S for "stagnant" (2).

$$W(\boldsymbol{v}) \coloneqq \begin{cases} 0 & , \frac{|\boldsymbol{v}|}{v_{\text{in}}} > 0.05 \\ 1 & , \frac{|\boldsymbol{v}|}{v_{\text{in}}} \leq 0.05 \end{cases} \tag{1}$$

$$S(\boldsymbol{v}) \coloneqq \frac{1}{V} \int_V W(\boldsymbol{v}) \, \mathrm{d}V \tag{2}$$

2.2.2 Minimize mixing variance

The reactor specifically aims for mixing in the cross-section to achieve near uniform concentration. Thus, variation of mixing should be minimized. We evaluate mixing by measuring the concentration c_{i} of a passive tracer substance which is added at the reactor inlet (cf. Figure 2). The mean concentration and variance of concentration are computed according to Equations (3) and (4). As objective function, we use the coefficient of variation CV,

which is the ratio of the square root of the variance to the mean (5). In the ideal case of a perfect mixture, CV would be equal to zero.

$$\text{Mean concentration:} \qquad \mathcal{E}(c_\mathrm{i}) \coloneqq \frac{1}{V}\int_V c_\mathrm{i}\,\mathrm{d}V \tag{3}$$

$$\text{Variance of concentration:} \qquad \mathcal{V}(c_\mathrm{i}) \coloneqq \frac{1}{V}\int_V \big(c_\mathrm{i} - \mathcal{E}(c_\mathrm{i})\big)^2\,\mathrm{d}V \tag{4}$$

$$\text{Coefficient of variance:} \qquad CV(c_\mathrm{i}) \coloneqq \frac{\sqrt{\mathcal{V}(c_\mathrm{i})}}{\mathcal{E}(c_\mathrm{i})} \tag{5}$$

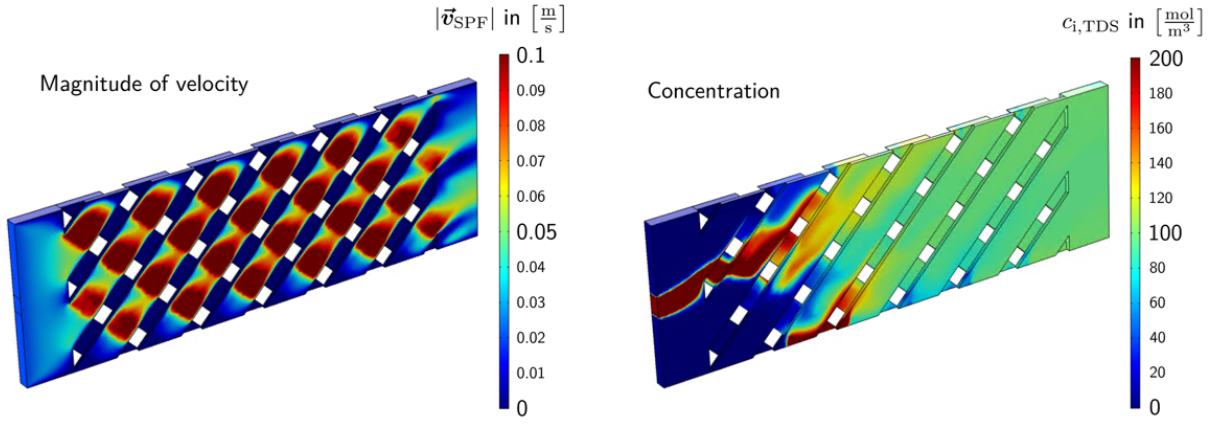

Figure 2: The flow field and concentration distribution for one of the reference geometries. (α=45°, d=1 mm, s=2 mm)

2.3 CFD setup

To keep the solution time of each individual CFD computation low, we introduce a number of simplifying assumptions. We assume the fluid passing through the reactor to be pure water at room temperature (20 °C). We consider a laminar, incompressible, isothermal steady-state flow. We model the mixing via a passive tracer, with the diffusion coefficient set to $1 \times 10^{-9}\,\mathrm{m}^2/\mathrm{s}$, corresponding to water-in-water diffusion. As the fluid properties remain constant at all times, we assume that the mixing does not have any effect on the fluid flow, but is affected by it.

In principle, Bayesian optimization can be used in tandem with any CFD solver. We use the commercial finite-element based software package COMSOL Multiphysics, version 5.1[34] to run the CFD simulations. We choose COMSOL because it is well suited for problems containing multiple phenomena, it has been already used in previous work[24], and it provides interfaces for coupling with external software (cf. Section 2.5).

We utilize Physics interfaces for laminar flow and transport of diluted species. We first compute the steady state flow field and in a transient second step the propagation of the tracer concentration. The simulation meshes consist of about 3×10^5 elements. For selected cases, we checked also the grid convergence. One simulation takes about 6.5 h on average using the default solver settings recommended by COMSOL.

2.4 Bayesian Optimization

Recall that Bayesian optimization is a technique for locating (near) global optimal solutions of a black-box objective function, meaning no information other than the function value, such as derivatives, are needed. The objective is treated as an arbitrary function captured by a stochastic model, which is updated iteratively as more data become available. Bayesian optimization is a data-efficient method suitable for dealing with expensive to evaluate functions, because it can efficiently draw probabilistic conclusions from analyzing a minimal amount of data[28]. In this work, we use the Thompson sampling efficient multiobjective optimization (TSEMO)[37] algorithm, which can handle multiple, conflicting objective functions. TSEMO uses Gaussian processes to build surrogate models of the objective functions. Then, TSEMO uses the cheap surrogate models to identify the most promising evaluation point for the next (expensive) function evaluation, a CFD simulation in our case. The CFD simulation is performed, evaluated, and the result used to update the surrogate models to find the new best evaluation point in an iterative fashion. Further, all simulations are added to the solution data set. While intermediate results are often discarded in other optimization methods, here they are incorporated to find, and may be part of, the Pareto frontier. The identification

of the most promising CFD simulations is done by a multi-objective genetic algorithm that optimizes random samples which are drawn from the Gaussian processes. Notably, this internal optimization problem could also be solved to global optimality using deterministic global methods[42]. Overall, TSEMO cannot provide guarantees of global solution but often determines a good approximation of the true Pareto front with significantly less iterations than genetic algorithms[36,37].

2.5 Coupling of CFD and optimization

To prepare the optimization cycle, the first step is the setup of the CFD case file template. The COMSOL Multiphysics graphical user interface is used to create the starting geometry, define the physics interfaces for fluid flow and species transport, and select the appropriate meshing and solver settings. The case file is then saved as a MATLAB (.m) file that contains all the information necessary to run the CFD simulation for the starting geometry. After this initial setup, COMSOL is only accessed via MATLAB through the LiveLink interface. The objective functions are implemented in MATLAB, and a set of initial geometry configurations is created consisting of reference configurations and configurations obtained via augmenting latin hypercube sampling (aLHS). For each configuration, a COMSOL case file is created starting from the template by modifying the respective geometry parameters. Next, the COMSOL simulations are run and the results evaluated via LiveLink[43]. These results form the initial data set used for the actual optimization. A Bayesian acquisition step is performed, using a stochastic model to determine new geometric parameters for the next CFD simulation. The results of this simulation in terms of the corresponding objective function values are added to the data set, and the cycle continues until a termination criterion is met. In this case, the optimization algorithm is stopped if a maximum number of iterations is reached.

3 Results and discussion

The aim of the Bayesian optimization algorithm was to efficiently find geometry configurations minimizing the objective functions S and CV. Starting from a data set containing the three reference configurations and seven additional configurations obtained via Latin hypercube sampling, the algorithm successively selected 70 further configurations to evaluate, for a total of 80 simulations. The simulations were run in series, the combined runtime was 22 days (wall time). The number of iterations (and thus also runtime) is orders of magnitude less than what a brute-force approach would require. For example, a reasonable grip would be 60 points for angle α (increments of 1°) and 20 points for each of the fin thickness d and distance s (increments of 0.1 mm) resulting in a total of 24,000 simulations.

The objective function values of the configurations are plotted in Figure 3. The blue crosses and green points denote the initial data set, the red circles the configurations chosen by the TSEMO algorithm. Most of the proposed geometries improve at least one of the objective function values significantly compared to the reference designs, with many improving both. Figure 4 shows a parallel coordinates plot of the the values of the geometric parameters with their corresponding objective function values. Each line in the plot represents one configuration, with the geometric parameter values plotted on the first three axes, and the objective values plotted on the middle-right and far-right axes. Thin lines mean the configurations are dominated, i.e. at least one other configuration improves both objective function values, and thick lines mean the configurations are dominating, i.e. Pareto-optimal. It is apparent that the mixing bar angle α seems to have the largest effect on the objective functions, with all dominating configurations featuring angles greater than 65°, whereas no clear preference can be assigned regarding the mixing element thickness d or distance s.

In the following, we examine three configurations more closely, and compare them to the reference configurations. These are the configurations yielding the least stagnant areas, i.e. the lowest value of the objective function S, the one with the best mixing, i.e. the lowest value of CV, and a Pareto-optimal tradeoff. For comparison, we take the reference

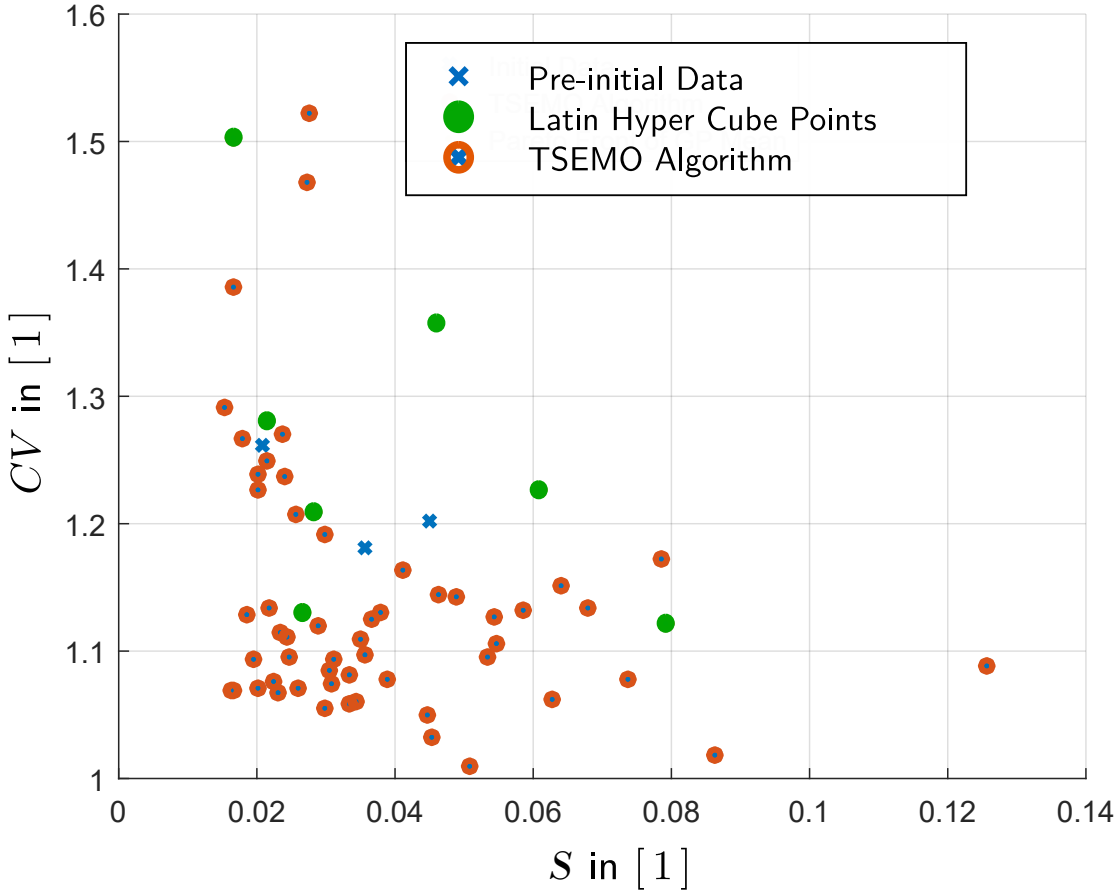

Figure 3: Objective function values of S and CV. The blue crosses and green points denote the initial data set, the red circles the configurations chosen by the TSEMO algorithm.

configurations with the best values of S and CV, respectively. They will be denoted S_{ref} and CV_{ref} henceforth. Table 1 gives the geometric parameters of the configurations and the corresponding absolute values of the objective functions S and CV, and Table 2 gives the relative improvements of the selected optimization results compared to S_{ref} and CV_{ref}.

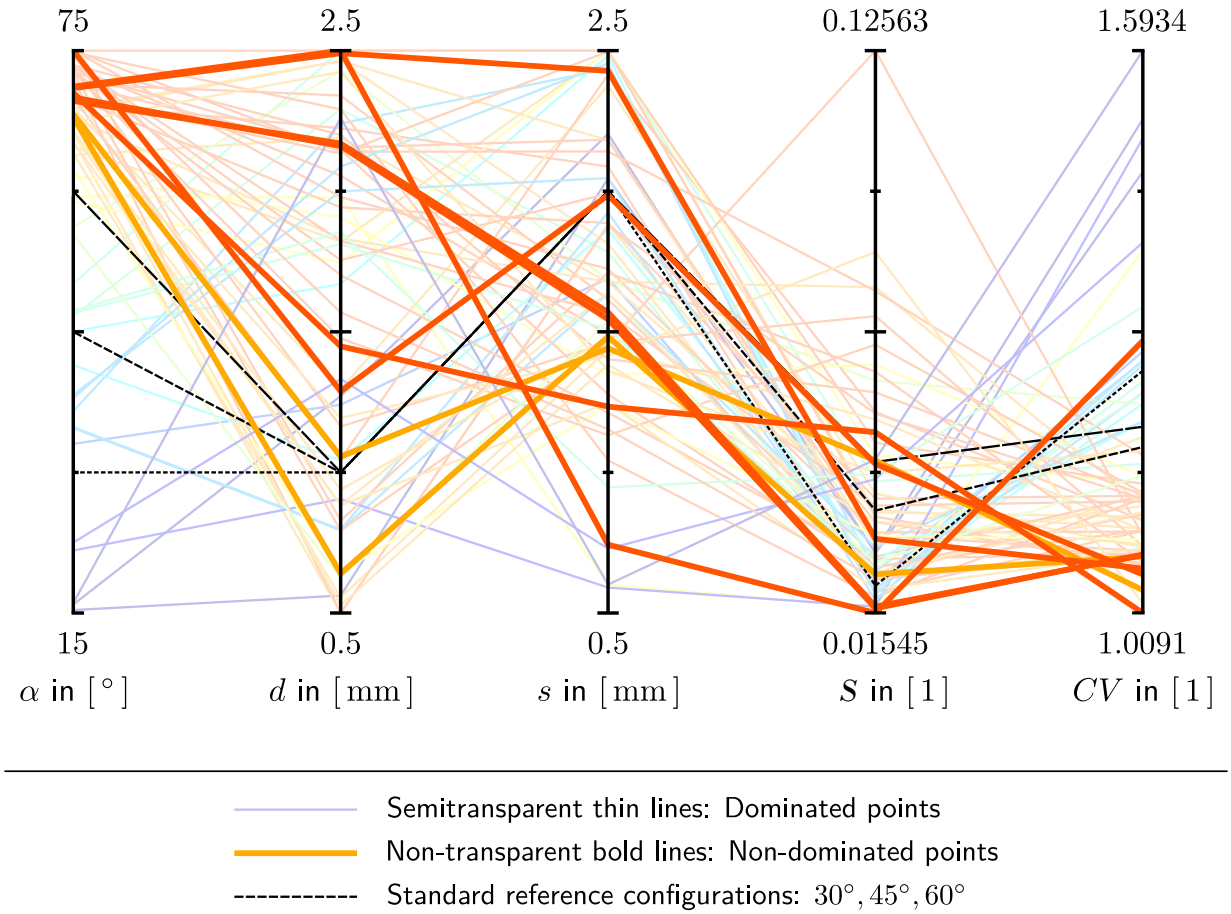

Figure 4: Parallel coordinates plot for α, d, s (cf. Figure 1) and the objectives S and CV. Every line in the plot corresponds to one simulated configuration, with color corresponding to the mixing bar angle α.

Table 1: Geometric parameters and objective function values of the three reference cases and selected optimization results.

	Configuration	α in [°]	d in [mm]	s in [mm]	S in [1]	CV in [1]
Reference	$\mathrm{Ref}_{30°} = S_{\mathrm{ref}}$	30	1	2	0.0208	1.2609
	$\mathrm{Ref}_{45°} = CV_{\mathrm{ref}}$	45	1	2	0.0355	1.1815
	$\mathrm{Ref}_{60°}$	60	1	2	0.0451	1.2025
TSEMO	S_{min}	71.16	2.5	0.74	0.0155	1.2918
	$(S/CV)_{\mathrm{tradeoff}}$	69.64	2.17	1.57	0.0167	1.0692
	CV_{min}	70.51	1.45	1.23	0.0509	1.0091

Table 2: Relative improvement/decrease of the objectives S and CV of the Bayesian optimization results with respect to the reference configurations S_{ref} and CV_{ref} (rounded).

... compared	to ...	ΔS_{rel}	ΔCV_{rel}	to ...	ΔS_{rel}	ΔCV_{rel}
S_{min}	S_{ref}	-26%	$+3\%$	CV_{ref}	-57%	$+9\%$
$(S/CV)_{\mathrm{tradeoff}}$	S_{ref}	-20%	-15%	CV_{ref}	-53%	-10%
CV_{min}	S_{ref}	$+145\%$	-20%	CV_{ref}	$+43\%$	-15%

3.1 Least stagnating flow areas

We show in Figure 5 the configuration leading to a minimal value of S.

Compared to S_{ref}, the stagnating flow areas are reduced by 26 %, while the mixing variance is increased by 3 %. The reduction of stagnating areas can be attributed to two factors. For one, the corners at the top and bottom of the reactor channel are well-aligned. Badly-aligned corner regions (cf. Figure 6) can form "dead zones", which have a heightened fouling potential. The second reason lies in the fact that the thickness of the mixing element fins d is at the maximum allowed value and the space between the fins s is rather small, leading to a reduction in the effective reactor volume and an increase of the average flow velocity.

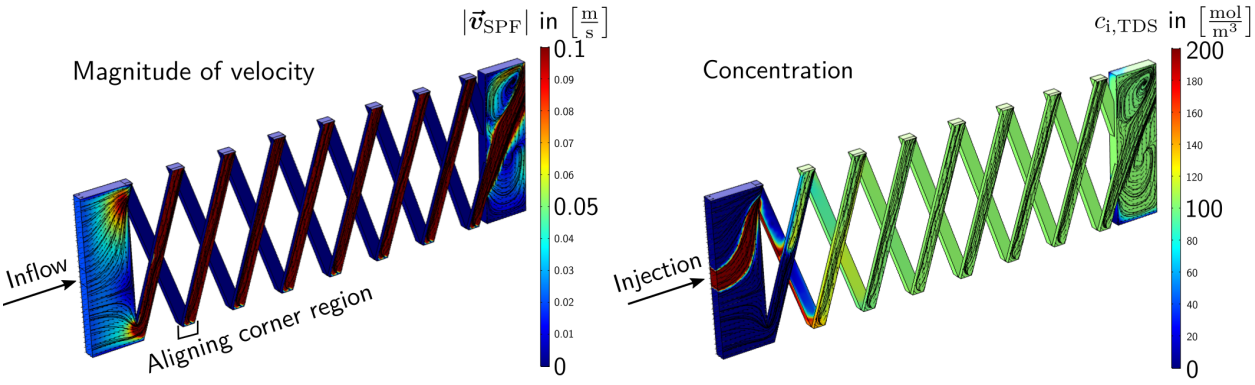

Figure 5: Configuration with the least stagnant areas. The geometric parameters are $\alpha = 71.16°$, $d = 2.5\,\mathrm{mm}$ and $s = 0.74\,\mathrm{mm}$.

3.2 Least mixing variance

Figure 6 shows the configuration yielding a minimum value of CV. Compared to CV_{ref}, the mixing variance is reduced by 15 %, while the stagnating areas are increased by 43 %.

Interestingly, while this configuration minimizes the mixing variance over the whole domain, the corner regions at the bottom of the channel are actually not that well mixed, indicating that it might be beneficial to give more weight to the top and bottom regions of the channel. Similarly, one might, e.g., neglect the first half of the channel to reduce the influence of the inlet section.

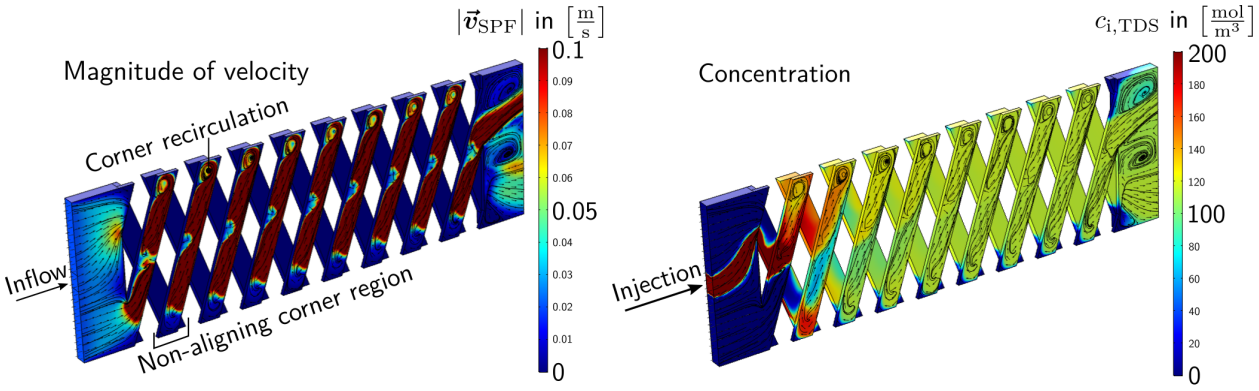

Figure 6: Configuration with the best mixing. The geometric parameters are $\alpha = 70.51°$, $d = 1.45\,\mathrm{mm}$ and $s = 1.23\,\mathrm{mm}$.

3.3 Pareto-optimal trade-off

The optimization algorithm was able to find eight configurations, including the two just discussed, which dominate all other tested configurations, and are assumed to be close to or on the true Pareto front. Due to the competing nature of the selected objective functions, no single configuration can claim to give the overall best result. Instead, a trade-off has to be selected by the user, depending on the specific requirements of the intended use-case.

Here, we select the configuration in the bottom-left corner of Figure 3, as its S value is still the second best found by the algorithm, and the corresponding CV value is drastically reduced compared to the S-optimal case. Figure 7 shows the results for this configuration. We observe that it reduces the stagnating flow areas by 19.7 % compared to S_{ref}, while still decreasing the mixing variance by 15.2 %. Compared to CV_{ref}, the stagnating flow areas are reduced by 53 %, and the mixing variance by 10 %. The configuration retains the aligned corners of the S-optimal case, but has a larger effective interior volume more in line with

the CV-optimal and reference configurations.

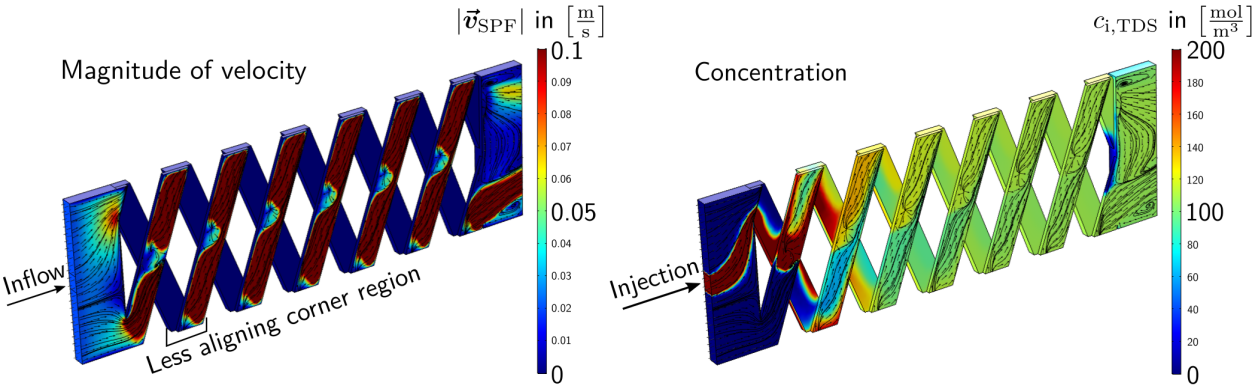

Figure 7: A tradeoff between the two objectives. The geometric parameters are $\alpha = 69.64°$, $d = 2.17\,\mathrm{mm}$ and $s = 1.57\,\mathrm{mm}$.

4 Conclusions

Continuous millireactors play an increasingly important role in the chemical industry. They are highly complex devices and their geometric optimization important. Numerical optimization can help to improve their designs, in additional to manual adjustments. We use the multi-objective Bayesian optimization algorithm TSEMO to generate improved geometry configurations for the Miprowa Lab millireactor. Two objective functions were optimized for, namely minimizing the stagnating flow areas and the mixing variance in the reactor. The proposed configurations yielded improvements compared to the best reference cases of up to 26 % and 15 percent, respectively. These results show that Bayesian optimization can be utilized successfully for geometry optimization of chemical reactors. The TSEMO algorithm used in this work is highly adaptable and can work with an arbitrary number of objective functions and parameters. It follows that, as long as the geometry can be suitably parameterized, the demonstrated method can be adapted to different devices and objective functions as required. While the results prove that the method is working as intended, they could be further improved by taking into account additional objectives or adapting the ones used. For example, the effect of the suggested modifications on the pressure loss was not of

interest here, but could be incorporated as an additional objective function. Similarly, the mixing variance was calculated over the whole reactor domain, potentially giving too much weight to the inlet area. Further work could attempt to explore the effects of, e.g., only evaluating the mixing quality in the second half of the reactor channel.

Acknowledgement

The work presented in this article was conducted as a part of the KoPPonA project, a research project concerned with the development of an efficient overall concept for continuously operated processes for specialty polymer production. The support of the German Federal Ministry for Economic Affairs and Energy (BMWi) under grant number 03ET1183C is gratefully acknowledged.

We thank Fabian Hübenthal for his support in running the optimization studies. Furthermore, we thank Frank Herbstritt of Ehrfeld Mikrotechnik GmbH for providing the reference geometries and for useful discussions.

References

(1) Gürsel, I. V.; Hessel, V.; Wang, Q.; Noël, T.; Lang, J. Window of opportunity – potential of increase in profitability using modular compact plants and micro-reactor based flow processing. *Green Process. Synth.* **2012**, *1*, 315–336.

(2) Brodhagen, A.; Grünewald, M.; Kleiner, M.; Lier, S. Increasing Profitability by Accelerated Product- and Process Development with Modular and Scalable Apparatuses. *Chem. Ing. Tech.* **2012**, *84*, 624–632.

(3) Jähnisch, K.; Hessel, V.; Löwe, H.; Baerns, M. Chemie in Mikrostrukturreaktoren. *Angew. Chem.* **2004**, *116*, 410–451.

(4) Illg, T.; Löb, P.; Hessel, V. Flow chemistry using milli- and microstructured reactors—From conventional to novel process windows. *Bioorg. Med. Chem.* **2010**, *18*, 3707 – 3719, Tetrahedron Young Investigator Award 2010: Professor SeebergerTetrahedron 2010.

(5) Calabrese, G. S.; Pissavini, S. From batch to continuous flow processing in chemicals manufacturing. *AIChE J.* **2011**, *57*, 828–834.

(6) Roberge, D. M.; Ducry, L.; Bieler, N.; Cretton, P.; Zimmermann, B. Microreactor Technology: A Revolution for the Fine Chemical and Pharmaceutical Industries? *Chem. Eng. Technol.* **2005**, *28*, 318–323.

(7) Sengen, A.-L.; Herbstritt, F.; Grünewald, M.; Heck, J. Experimental Investigation of the Convective Heat Transfer Coefficient in a Rectangular Microchannel. *Chem. Ing. Tech.* **2017**, *89*, 379–389.

(8) Roberge, D.; Noti, C.; Irle, E.; Eyholzer, M.; Rittiner, B.; Penn, G.; Sedelmeier, G.; Schenkel, B. Control of Hazardous Processes in Flow: Synthesis of 2-Nitroethanol. *J. Flow Chem.* **2014**, *4*, 26–34.

(9) Biessey, P.; Grünewald, M. Influence of Design Parameters on Hydrodynamics and Heat Transfer of a Modularized Millireactor. *Chem. Eng. Technol.* **2015**, *38*, 602–608.

(10) Hartman, R. L. Managing Solids in Microreactors for the Upstream Continuous Processing of Fine Chemicals. *Org. Process Res. Dev.* **2012**, *16*, 870–887.

(11) Schoenitz, M.; Grundemann, L.; Augustin, W.; Scholl, S. Fouling in microstructured devices: a review. *Chem. Commun.* **2015**, *51*, 8213–8228.

(12) Mitsos, A.; Palou-Rivera, I.; Barton, P. I. Alternatives for Micropower Generation Processes. *Ind. Eng. Chem. Res.* **2004**, *43*, 74–84.

(13) Mitsos, A.; Chachuat, B.; Barton, P. I. Methodology for the Design of Man-Portable Power Generation Devices. *Ind. Eng. Chem. Res.* **2007**, *46*, 7164–7176.

(14) An, H.; Li, A.; Sasmito, A. P.; Kurnia, J. C.; Jangam, S. V.; Mujumdar, A. S. Computational fluid dynamics (CFD) analysis of micro-reactor performance: Effect of various configurations. *Chem. Eng. Sci.* **2012**, *75*, 85 – 95.

(15) Woldemariam, M.; Filimonov, R.; Purtonen, T.; Sorvari, J.; Koiranen, T.; Eskelinen, H. Mixing performance evaluation of additive manufactured milli-scale reactors. *Chem. Eng. Sci.* **2016**, *152*, 26 – 34.

(16) Schönfeld, F.; Hardt, S. Simulation of helical flows in microchannels. *AIChE J.* **2004**, *50*, 771–778.

(17) Shi, X.; Xiang, Y.; Wen, L.-X.; Chen, J.-F. CFD Analysis of Flow Patterns and Micromixing Efficiency in a Y-Type Microchannel Reactor. *Ind. Eng. Chem. Res.* **2012**, *51*, 13944–13952.

(18) Buchelli, A.; Call, M. L.; Brown, A. L.; Bird, A.; Hearn, S.; Hannon, J. Modeling Fouling Effects in LDPE Tubular Polymerization Reactors. 2. Heat Transfer, Computational Fluid Dynamics, and Phase Equilibria. *Ind. Eng. Chem. Res.* **2005**, *44*, 1480–1492.

(19) Amini, E.; Mehrnia, M. R.; Mousavi, S. M.; Mostoufi, N. Experimental Study and Computational Fluid Dynamics Simulation of a Full-Scale Membrane Bioreactor for Municipal Wastewater Treatment Application. *Ind. Eng. Chem. Res.* **2013**, *52*, 9930–9939.

(20) Brahim, F.; Augustin, W.; Bohnet, M. Numerical simulation of the fouling process. *Int. J. Therm. Sci.* **2003**, *42*, 323 – 334.

(21) Rahimi, M.; Madaeni, S.; Abolhasani, M.; Alsairafi, A. A. CFD and experimental

studies of fouling of a microfiltration membrane. *Chem. Eng. Process.* **2009**, *48*, 1405 – 1413.

(22) Gobert, S. R. L.; Kuhn, S.; Braeken, L.; Thomassen, L. C. J. Characterization of Milli- and Microflow Reactors: Mixing Efficiency and Residence Time Distribution. *Org. Process Res. Dev.* **2017**, *21*, 531–542.

(23) Rodríguez-Guerra, Y.; Gerling, L. A.; López-Guajardo, E. A.; Lozano-García, F. J.; Nigam, K. D. P.; Montesinos-Castellanos, A. Design of Micro- and Milli-Channel Heat Exchanger Reactors for Homogeneous Exothermic Reactions in the Laminar Regime. *Ind. Eng. Chem. Res.* **2016**, *55*, 6435–6442.

(24) Begall, M. J.; Krieger, A.; Recker, S.; Herbstritt, F.; Mhamdi, A.; Mitsos, A. Reducing the Fouling Potential in a Continuous Polymerization Millireactor via Geometry Modification. *Industrial & Engineering Chemistry Research* **2018**, *57*, 6080–6087.

(25) Morita, Y.; Rezaeiravesh, S.; Tabatabaei, N.; Vinuesa, R.; Fukagata, K.; Schlatter, P. Applying Bayesian optimization with Gaussian process regression to computational fluid dynamics problems. *Journal of Computational Physics* **2022**, *449*, 110788.

(26) Towara, M.; Naumann, U. A Discrete Adjoint Model for OpenFOAM. *Procedia Computer Science* **2013**, *18*, 429–438, 2013 International Conference on Computational Science.

(27) Hannemann-Tamas, R.; Tillack, J.; Schmitz, M.; Förster, M.; Wyes, J.; Nöh, K.; von Lieres, E.; Naumann, E.; Wiechert, W.; Marquardt, W. First- and Second-Order Parameter Sensitivities of a Metabolically and Isotopically Non-Stationary Biochemical Network Model. 2012; pp 641–648.

(28) Brochu, E.; Cora, V. M.; de Freitas, N. A Tutorial on Bayesian Optimization of Expensive Cost Functions, with Application to Active User Modeling and Hierarchical Reinforcement Learning. *CoRR* **2010**, *abs/1012.2599*.

(29) Coppedè, A.; Gaggero, S.; Vernengo, G.; Villa, D. Hydrodynamic shape optimization by high fidelity CFD solver and Gaussian process based response surface method. *Applied Ocean Research* **2019**, *90*, 101841.

(30) Zuhal, L. R.; Amalinadhi, C.; Dwianto, Y. B.; Palar, P. S.; Shimoyama, K. *2018 AIAA/ASCE/AHS/ASC Structures, Structural Dynamics, and Materials Conference*.

(31) Park, S.; Na, J.; Kim, M.; Lee, J. M. Multi-objective Bayesian optimization of chemical reactor design using computational fluid dynamics. *Computers & Chemical Engineering* **2018**, *119*, 25–37.

(32) Cho, S.; Kim, M.; Lee, J.; Han, A.; Na, J.; Moon, I. Multi-objective optimization of explosive waste treatment process considering environment via Bayesian active learning. *Engineering Applications of Artificial Intelligence* **2023**, *117*, 105463.

(33) Park, S.; Atwair, M.; Kim, K.; Lee, U.; Na, J.; Zahid, U.; Lee, C.-J. Bayesian optimization of industrial-scale toluene diisocyanate liquid-phase jet reactor with 3-D computational fluid dynamics model. *Journal of Industrial and Engineering Chemistry* **2021**, *98*, 327–339.

(34) COMSOL Multiphysics v. 5.1 release website. `https://www.comsol.com/release/5.1`.

(35) Introduction to COMSOL Multiphysics v. 5.1. `https://cdn.comsol.com/doc/5.1/IntroductionToCOMSOLMultiphysics.pdf`.

(36) Thompson sampling efficient multiobjective optimization. `https://github.com/Eric-Bradford/TS-EMO`.

(37) Bradford, E.; Schweidtmann, A. M.; Lapkin, A. Efficient multiobjective optimization employing Gaussian processes, spectral sampling and a genetic algorithm. *Journal of Global Optimization* **2018**, *71*, 407–438.

(38) Ehrfeld Mikrotechnik Miprowa Flyer. 2018; https://ehrfeld.com/fileadmin/user_upload/Ehrfeld_Flyer_Miprowa_2018_D.pdf.

(39) Pfenning, D.; Kleiber, M. ACHEMA-Nachbericht: Prozesstechnik auf der ACHEMA 2015. *Chem. Ing. Tech.* **2015**, *87*, 1454–1464.

(40) Ehrfeld Mikrotechnik website. https://www.ehrfeld.com.

(41) Kukulka, D. J.; Devgun, M. Fluid temperature and velocity effect on fouling. *Appl. Therm. Eng.* **2007**, *27*, 2732 – 2744.

(42) Schweidtmann, A. M.; Bongartz, D.; Grothe, D.; Kerkenhoff, T.; Lin, X.; Najman, J.; Mitsos, A. Deterministic global optimization with Gaussian processes embedded. *Mathematical Programming Computation* **2021**, *13*, 553–581.

(43) COMSOL Multiphysics LiveLink website. https://www.comsol.com/livelink-for-matlab.